Semihard collisions in Monte Carlo quark-gluon string model

N. S. Amelin
Physics Department, University of Bergen, Allégaten 55, N-5007 Bergen, Norway

E. F. Staubo
NORDITA, Blegdamsvej 17, DK-2100 Copenhagen Ø, Denmark

L. P. Csernai
Physics Department, University of Bergen, Allégaten 55, N-5007 Bergen, Norway
and Theoretical Physics Institute, University of Minnesota, 116 Church Street SE, Minneapolis, Minnesota 55455
(Received 14 November 1991)

The production of parton cascades, i.e., the hard parton scatterings with their subsequent decay, is introduced in the Monte Carlo quark-gluon string model. The influence of the semihard gluon collisions on observable characteristics of proton-antiproton interactions at energies reached at the CERN Super Proton Synchrotron and Fermilab Tevatron is examined within the eikonal approach allowing us to combine the soft and semihard gluon collisions.

PACS number(s): 12.40.Aa, 12.40.Lk, 13.85.Hd

I. INTRODUCTION

Up to now, high-energy hadronic physics has been divided into high- and low-p_t parts. We lack a unified quantitative description of high- and low-tranverse-momentum phenomena in hadronic collisions. High p_t, or hard parton scattering, is able to account for many different aspects of hadronic collisions at existing collider energies [1], and their role increases with increasing energy. Scattering with large momentum transfer can be described by perturbative quantum chromodynamics (QCD) in terms of colored partons. The commonly used Monte Carlo algorithms for this purpose [2,3] are combinations of Q^2-dependent structure functions, where Q^2 characterizes the "hardness" of the parton-parton scattering, and lowest-order hard-parton-scattering matrix elements with initial- and final-state coherent parton shower evolution.

At available energies, low-p_t phenomena by far constitute the most important contribution to the total hadron collision cross section, and multiple production of hadrons is mainly associated with them. But an effective low-transverse-momentum theory has not been derived from QCD. However, many results point to the fact that open relativistic one-dimensional strings play an essential role [4]. At present, the popular phenomenological description of multiple-particle production in hadron and nuclear collisions is based on the assumption that hadron production is the result of the creation and decay of open strings with different quarks at their ends. There are numerous versions of the two QCD-motivated approaches: the Fritiof model [5,6] and the dual parton model (DPM) [7–15], which use different mechanisms for string excitation. Practically all of them are formulated as Monte Carlo event generators, allowing one to perform a careful analysis of the measurable quantities by introducing all necessary experimental cuts.

In earlier papers [16], a Monte Carlo version of the DPM for low-p_t hadron-hadron collisions was developed, called the quark-gluon string model (QGSM). The name is borrowed from Kaidalov *et al.* [9,11], and we have used the same statistical weights, hadron structure functions, and leading quark fragmentation functions (obtained from the Regge approach) to choose subprocesses of string production, to compute the mass and momentum of strings and to simulate string decays.

This model was extended to describe hadron-nucleus and nucleus-nucleus collisions [17]. The QGSM [16] predicts correctly many of the high-energy features for proton-antiproton collisions at collider energies, such as the long-range correlations, the Koba-Nielsen-Olesen (KNO) scaling violation for charged multiplicity, and the rise of the rapidity plateau as a function of initial energy. These features are determined by multicolor exchanges which are not accompanied by momentum transfer. They are so-called soft parton collisions, leading to the production of pairs of strings.

Recently, there have been attempts to extend the high- and low-p_t models to describe the entire p_t range. In the case of the DPM approach, the basic role in this extension is played by the perturbative, but not very hard—the so-called semihard [18,19]—parton collisions, which can be responsible for a rise of the hadronic cross section at high energies. The authors of [20–22] formulated the eikonal model to explain a rise of the total and inelastic cross sections by a combination of the soft and semihard gluon scatterings. A Monte Carlo version of the DPM, which includes both soft and semihard parton collisions, but disregarding gluon radiation, was developed by Hahn and Ranft [23].

In Refs. [24,25] one can find attempts to formulate a parton cascade model, where partons are allowed to propagate, decay, and rescatter, for the investigation of ultrarelativistic heavy-ion collisions.

We wish to include these effects into the QGSM in order to describe heavy-ion collisions at energies reached at the BNL Relativistic Heavy Ion Collider (RHIC) and CERN Large Hadron Collider (LHC), and proton reactions at energies reached at the Fermilab Tevatron. Including hard parton cascades in the QGSM has the advantage that we can utilize the well-worked-out hadronization procedure in this model. This hadronization is via string or cluster formation and decay. Our present model formulation of hard parton scatterings should be regarded as a first step on the way to inserting parton cascades in an explicit manner into the QGSM devoted to ultrarelativistic hadron and nucleus collisions.

In the first part of this paper, we introduce hard parton scattering and parton decay in the Monte Carlo QGSM [16]. This is accomplished in a well-known way [2,3], which is adapted to take into account the propagation of partons, before their decay or hadronization.

In the second part, we wish to examine the efficiency of the model and the influence of semihard gluon collisions on observable characteristics of proton-antiproton interactions at energies reached at the CERN Super Proton Synchrotron (SPS) [26] and Tevatron [27,28]. In particular, we focus on the strong correlation between the mean transverse momentum of the produced particles and their multiplicity observed in hadron collision experiments [26–29]. We also analyze the strangeness enhancement and antibaryon production observed in $\bar{p}p$ at $\sqrt{s}=1800$ GeV [28]. These observables were suggested [30,31] as signals of a phase transition to a quark-gluon plasma (QGP).

II. PARTON CASCADES

In our model virtual partons defined by their invariant mass squared M^2 are at first created in hard collisions. They may decay into other partons and initiate parton cascades. At this stage we do not consider possible rescatterings of partons from different cascades.

If M^2 is positive (negative), we speak about timelike (spacelike) virtual partons. The final partons emerging from the hard scattering are timelike since they evolve from a virtuality $M^2>0$, and their secondaries are allowed to decay down to a cutoff value M_c^2.

For partons originating from the initial projectile and target nucleons, a hard scattering at momentum scale Q^2 should be preceded by a parton decay that changes the initial small spacelike virtuality of the incident parton ($M^2\approx -M_c^2$) down to a virtuality close to the momentum scale of the hard scattering in an absolute value $M^2\approx -Q^2$.

In our present model, however, this spacelike branching is not treated explicitly. Instead, we use Q^2-dependent structure functions which include the effects of partons of negative virtuality.

We have also neglected coherence effects during the timelike parton evolution (see Ref. [32]), which leads to angular ordering of radiated gluons for two subsequent decays. This can be justified in our case, because we limit the calculations to semihard gluon rescatterings with relatively small virtualities of outgoing partons. Our outgoing partons radiate as a rule only one gluon. In the case of truly hard parton scattering, we would have to take into account the coherence of gluon radiation, since we use a low mass-squared cutoff M_c^2 to stop the parton decay.

Partons with virtuality degraded to M_c^2 form hadrons via cluster formation with another parton (see below).

A. Creation of virtual partons in hard scatterings

We will consider $2\rightarrow n$ parton processes. We adopt the parton shower (cascade) approach [2,3], in which the $2\rightarrow n$ parton process is subdivided into a hard-scattering $2\rightarrow 2$ subprocess and final-state (timelike) parton cascades.

Our sampling of hard parton-parton interactions is based on the two-jet inclusive cross section [33], which may be written as a sum of terms, each representing a given contribution to the cross section due to a particular combination of incoming partons i,j ($i,j=g,q$) with momenta p_1 and p_2 and outgoing virtual partons k,l with momenta p_3 and p_4:

$$\frac{d\sigma}{dy_3 dy_4 dp_t^2}=\frac{\pi}{\hat{s}}\sum_{ij\rightarrow kl} f_i(x_1,Q^2)f_j(x_2,Q^2) \times\frac{1}{x_1x_2}\frac{d\hat{\sigma}_{ij\rightarrow kl}}{d\hat{t}}\frac{1}{1+\delta_{ij}} . \quad (1)$$

where $\hat{\sigma}_{ij\rightarrow kl}/d\hat{t}$ are the differential cross sections of subprocesses of quarks and/or gluons, computed as in Ref. [34] for massless quarks, $\delta_{i,j}$ is the Kronecker delta, and $f_{i,j}(x_{1,2},Q^2)$ are the structure functions evaluated at momentum scale Q^2. They give the probability for finding partons i,j carrying fractions $x_{1,2}$ of the initial energy and longitudinal momentum of the incoming hadrons. The choice of structure functions and other parameters is discussed in Sec. IV A.

The differential cross section $\hat{\sigma}_{ij\rightarrow kl}/d\hat{t}$ depends on the Mandelstam variables $\hat{s}=(p_1+p_2)^2$, $\hat{t}=(p_3-p_1)^2$, and $\hat{u}=(p_4-p_1)^2$. We used the algorithm described in Ref. [3] to obtain the rapidities of outgoing partons, y_3 and y_4, and their transverse momenta p_t. Since the parton cross sections diverge for $p_t\rightarrow 0$, we have introduced a cutoff at $p_t^{\min}$.

To attach timelike parton cascades to the $2\rightarrow 2$ process of hard parton scattering, we give k and l maximum virtuality: If a parton with mass m_1 scatters on a parton of mass m_2 into parton 3 and 4, the maximum virtualities $M_{3,4}^2$ for the outgoing partons 3 and 4 are the maximum invariant masses possible for partons 3 and 4 in the center-of-mass system (c.m.s.) of initial partons 1 and 2, given by

$$M_{3,4}^4+2M_{3,4}^2(m_{1,2}^2-\sqrt{\hat{s}}E_{1,2}-\hat{t}+2\mathbf{p}_{1,2}^2) +(\hat{t}+\sqrt{\hat{s}}E_{1,2}-m_{1,2}^2)^2-\hat{s}\mathbf{p}_{1,2}^2=0 , \quad (2)$$

In (2), $E_{1,2}=p_{1,2}^0$ and $\mathbf{p}_{1,2}$ are the energy and momentum of parton 1 or 2 in the c.m.s. of partons 1 and 2 correspondingly.

B. Parton decay

We simulated parton decay using the Fox-Wolfram algorithm [35,36]. The probability that a parton of type j and invariant mass squared M_j^2 decays into partons of types j_1 and j_2 carrying fractions z and $(1-z)$, respectively, of the summed energy and momentum of parton j is given by

$$dP=\frac{\alpha_s(M_j^2)}{2\pi M_j^2}P_{j\to j_1 j_2}(z)dz\,dM_j^2 \ . \tag{3}$$

Here

$$\alpha_s(Q^2)=\frac{4\pi}{\beta_0\ln(Q^2/\Lambda^2)} \tag{4}$$

is the QCD effective coupling, $\beta_0=11-\frac{2}{3}n_f$, where $n_f=3$, and $P_{j\to j_1 j_2}(z)$ are the Altarelli-Parisi [37] splitting probability functions. The splitting function for a gluon splitting into q and $\bar{q}$ is

$$P_{g\to q\bar{q}}(z)=\tfrac{1}{2}[z^2+(1-z)^2] \ . \tag{5}$$

Similarly, the other splitting functions are

$$P_{g\to gg}(z)=6\frac{[1-z(1-z)]^2}{z(1-z)} \ , \tag{6}$$

$$P_{q\to qg}(z)=\frac{4}{3}\frac{1+z^2}{1-z} \ . \tag{7}$$

The probability π_j that parton j of invariant mass squared M_j^2 decays only into parton j of invariant mass squared M_c^2 and "unresolvable" soft partons is

$$\pi_j(M_j^2,M_c^2)=\left[\frac{\alpha_s(M_j^2)}{\alpha_s(M_c^2)}\right]^{d_j} \ , \tag{8}$$

$$d_j=2\gamma_j(z_c)/\beta_0 \ , \tag{9}$$

$$\gamma_j(z_c)=\int_{z_c}^{1-z_c}P_{j\to \text{all}}(z)dz \ . \tag{10}$$

Here z_c is determined from the equation $z_c(1-z_c)M_j^2=M_c^2$. Thus, in a "resolvable" decay, the splitting variable z at the outgoing parton should fall in the range $z_c>z>1-z_c$. This probability (8) is used to decide if there will or will not be a "resolvable" decay of the jth parton. In case of an "unresolved" decay or a decay without radiation, we have $M_j^2=M_c^2$, and the process of evolution is stopped. If there is a "resolved" decay, we choose the mass squared $M_{j_{1,2}}^2$ according to

$$f(M_j^2,M_{j_{1,2}}^2)=\frac{\alpha_s(M_{j_{1,2}}^2)}{2\pi M_{j_{1,2}}^2}\gamma_j(z_c)\pi_j(M_j^2,M_{j_{1,2}}^2) \ . \tag{11}$$

The values of z are obtained from the splitting functions $P_{j\to j_1 j_2}(z)$. Further details of the decay algorithm can be found in [35,36].

In the described probabilistic approach, the successive decay processes correspond to decreasing values of the square of the parton mass squared M_j^2. The time of life, Δt_j, of a virtual parton j is determined by the parton mass squared M_j^2 as

$$\Delta t_j\sim 1/\Delta E=(E+|\mathbf{p}|)/M_j^2 \ . \tag{12}$$

Here E and $|\mathbf{p}|$ are the energy and momentum of the parton. The virtual parton can propagate during its time of life until its decay or possible rescattering [38,24]. At the end all partons end up in a cluster or string leading to hadronization.

C. Parton hadronization

Partons with $M_j^2<M_c^2$ are considered for hadronization. Before hadronization, we transform each gluon into a $\bar{q}q$ pair with the probability [Eq. (5)] to compute the angular distribution of quarks, although this is strictly valid only in the perturbative case. The final partons in a cascade, except (i) in the case of a parton cascade initiated by a quark or (ii) in the case of a parton cascade initiated by a gluon, can be matched to build colorless strings or clusters [38–40]. Most strings, if we choose a low mass cutoff M_c, will have small masses. We call such strings "clusters" to stress their isotropic angular decay into two hadrons in their c.m. The breakup of strings and clusters was described in earlier papers on the QGSM [16]. After the secondaries are determined, their space-time formation point is calculated according to the constituent formation time definition [41,17].

If we have two or more sources for the parton cascades, as considered below for inelastic hadron collisions, there may be many scenarios (see Ref. [42]) to connect the nonmatched color charge. In general, this poses a difficult problem, but for the purpose of our investigation, it may be simplified.

III. HIGH-ENERGY PROTON-ANTIPROTON COLLISIONS

Here we will consider inelastic proton-antiproton collisions, when one or more hard and soft scatterings can occur. We assume only hard gluon-gluon scatterings of the $gg\to gg$ or $gg\to\bar{q}q$ type with the two gluons in a color-singlet state. This simplification allows us to combine in a unique way the nonmatched final quarks into strings or clusters and decouple hard scatterings from the rest of the system with the soft string creations. Initially, we simulate the hard gluon-gluon scatterings. Then the momentum and energy of the hard scattering is subtracted and we simulate the soft collisions, for which we use the earlier QGSM version [16].

An example of the colorless string or cluster creation algorithm in the case of a $\bar{p}p$ collision with two hard gluon-gluon scatterings and their connection with the soft process is presented in Fig. 1.

To obtain the number of soft quark and semihard parton (in this case gluon) collisions in each hadron nondiffractive inelastic scattering, we used the eikonal approach [21,22]. In the eikonal formalism [20–22], the inelastic hadron-hadron cross section $\sigma_{\text{in}}(s)$ is expressed as

$$\sigma_{\text{in}}(s)=\pi\int_0^\infty db^2[1-\exp(-2u)] \ , \tag{13}$$

via the eikonal $u(s,b)$, which is a function of the square of the c.m.s. energy s and the impact parameter of colliding hadrons, b.

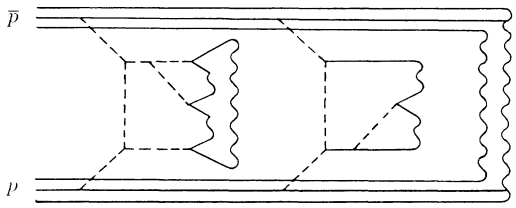

FIG. 1. Creation of strings in two semihard and one soft subprocesses for $p\bar{p}$ interactions. Solid lines correspond to quarks and antiquarks, dashed lines correspond to gluons, and wavy solid lines mean colorless strings or clusters.

Following Ref. [21], we consider the eikonal $u(s,b)$ with three driving terms: the soft Pomeron, the semihard Pomeron, and the triple Pomeron terms:

$$u(s,b)=u_{\text{soft}}(s,b)+u_{\text{hard}}(s,b)+u_{\text{triple}}(s,b) . \tag{14}$$

The triple Pomeron term is included in the eikonal expression, because it is responsible for the single-diffraction process (σ_{SD}). We will not calculate diffraction in this paper, but to compute the soft-collision probability, we need this term.

In this eikonal model, the elastic-hadron-scattering amplitude can be represented as a sum of diagrams with the soft, semihard, and triple Pomeron exchanges. Some cuts of these diagrams lead to inelastic hadron interactions, one of which is shown in Fig. 1, with the soft gluon scattering and two hard gluon scatterings subprocesses correspondingly.

Compared with Ref. [22], we neglect the loop Pomeron term in the eikonal $u(s,b)$, some cuts of which lead to a double-diffractive processes.

Then the inelastic cross section $\sigma_{\text{in}}(s)$ of hadron scattering can be presented by the expression

$$\sigma_{\text{in}}(s)=\sigma_{\text{ND}}(s)+\sigma_{\text{SD}}(s) , \tag{15}$$

where $\sigma_{\text{ND}}(s)$ is the nondiffractive inelastic cross section and σ_{SD} is the single-diffractive one. The nondiffractive inelastic proton-antiproton scattering can be divided into soft and semihard components.

Substituting (14) into (13), we can split up the nondiffractive inelastic cross section into soft and hard components:

$$\sigma_{\text{ND}}=\sigma_{\text{soft}}+\sigma_{\text{hard}} , \tag{16}$$

$$\sigma_{\text{soft}}(s)=\pi\int_0^\infty db^2[1-\exp(-2u_{\text{soft}})] \times\exp(-2u_{\text{hard}})\exp(-2u_{\text{triple}}) , \tag{17}$$

$$\sigma_{\text{hard}}(s)=\pi\int_0^\infty db^2[1-\exp(-2u_{\text{hard}})] . \tag{18}$$

The $[1-\exp(-2u_{\text{hard}})]$ term is the probability of hard scattering at the impact parameter b, whether or not it is accompanied by soft production and diffraction. In the proton-antiproton case, the eikonals can be expressed via the soft and hard Pomeron parameters, as was done in Refs. [21,22]:

$$u_{\text{soft(hard)}}(s,b)=z_{\text{soft(hard)}}(s)\exp[-b^2/4\lambda_{\text{soft(hard)}}(s)] . \tag{19}$$

The values $z_{\text{soft(hard)}}(s)$ and $\lambda_{\text{soft(hard)}}(s)$ are determined by Pomeron trajectory parameters α'_P and $\alpha_P(0)$ and Pomeron-nucleon vertex parameters R_P^2 and γ_P as

$$z_{\text{soft(hard)}}(s)=\frac{\gamma_P}{\lambda(s)}\left[\frac{s}{s_0}\right]^{\alpha_P(0)-1} \tag{20}$$

and

$$\lambda_{\text{soft(hard)}}(s)=R_P^2+\alpha'_P\ln\left[\frac{s}{s_0}\right] , \tag{21}$$

where s_0 is a scale parameter.

To find the number i of parton collisions of type T (T = soft and semihard), we used the probability

$$P_{i,T}(s,b)=\frac{[2u_T(s,b)]^i}{i!}\exp[-2u_T(s,b)] . \tag{22}$$

IV. COMPARISON WITH EXPERIMENTAL DATA

A. Choice of parameters

In Eqs. (19)–(21) we have taken the soft and hard Pomeron parameters from Refs. [21,22], which were obtained from a global fit to the total, elastic, single-diffractive, and minijet cross sections as functions of energy. For the chosen soft and hard Pomeron parameters, we show in Fig. 2 the mean numbers of soft and semihard collisions inside a nucleon at $\sqrt{s}=1.8$ TeV as a function of the impact parameter. The pure hard Pomeron cross section which was used to compute the parameters of hard Pomerons was evaluated in Ref. [21] in perturbative QCD at $p_t^{\min}\approx 2.5$ GeV/c. We used this value for sampling gluon-gluon hard scatterings. We have chosen set 1 for $F(x,Q^2)=f(x,Q^2)/x$ from Ref. [33], with $\Lambda=0.2$ GeV and a momentum scale $Q^2=p_t^2$.

In case of several semihard collisions, we should use the joint probability distribution to find gluons with

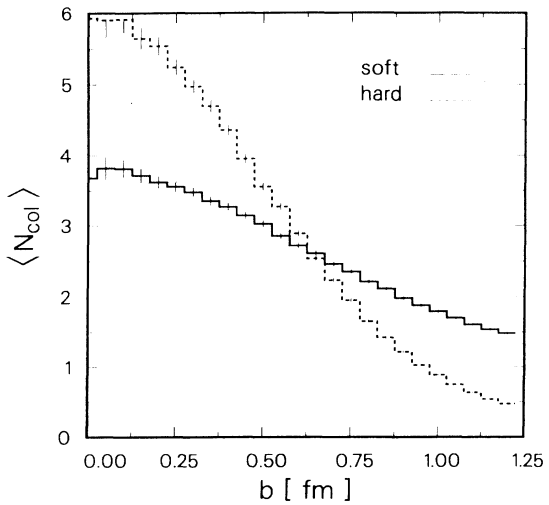

FIG. 2. Mean number of soft (solid histogram) and semihard (dashed histogram) collisions as a function of the impact parameter in inelastic $p\bar{p}$ interactions at $\sqrt{s}=1800$ GeV.

different x. Here we only use the ordinary structure function, but take into account the energy and longitudinal momentum spent in previous semihard scattering, by the procedure devised in Ref. [19]. We evaluated the structure function for the nth scattered gluon from protons or antiprotons not at x_n, but at

$$x_n' = \frac{x_n}{1-\sum_{i=1}^{n-1} x_i} \ . \tag{23}$$

Cascade parton decay was stopped by the cutoff for a virtual parton mass squared $M_c^2 \approx 1$ GeV^2.

To avoid production of clusters with too low mass, which cannot decay into hadrons, we used the on-shell quark masses $M_u = M_d = 0.3$ GeV and $M_s = 0.5$ GeV for u, d, and s quarks correspondingly.

To calculate the kinematical parameters of strings produced in soft collisions, we used the phenomenological structure functions taken from Ref. [9]. For incoming nucleons consisting of valence quarks, valence diquarks, and sea quarks, we used the joint structure function

$$f(x_1,x_2,\ldots,x_{2n}) = f_0 \delta\left[1-\sum_{i=1}^{2n} x_i\right] \times f_{V_1}(x_1) f_S(x_2)\cdots f_{V_2}(x_{2n}) \ , \tag{24}$$

where f_0 is a normalization constant. This determines the fraction x_i of the initial hadron energy and longitudinal momentum that is carried away by the parton i participating in the string formation. The distribution function of the valence quark, $f_{V_1}(x_1)$, diquark, $f_{V_2}(x_{2n})$, and sea quarks, $f_S(x_2)$, in the nucleon are

$$\begin{aligned} f_{V_1}(x_1) &= \frac{1}{\sqrt{x_1}} \ , \\ f_S(x_2) &= x_2^{\beta_1} \ , \\ f_{V_2}(x_{2n}) &= x_{2n}^{\beta_2} \ . \end{aligned} \tag{25}$$

The δ function in Eq. (24) takes into account that the constituents carry away the whole nucleon momentum. The exponent β_1 is -0.5 for nonstrange sea quarks and 0 for strange sea quarks. The exponent β_2 is 1.5 for a uu diquark and 2.5 for a ud diquark inside a proton.

For the transverse momentum distribution of quarks in hadrons, strict theoretical predictions do not yet exist. The primordial transverse momentum of a quark in this case was generated according to

$$f_1(\mathbf{p}_t) = \frac{b_1}{\pi} \exp(-b_1 p_t^2) \ . \tag{26}$$

By using this distribution function, transverse momenta of all quarks, except for diquarks in the nucleon, were generated independent of each other. The diquark transverse momentum was equal in magnitude, but of opposite direction. The parameter b_1 was chosen as $b_1 = 3$ (GeV/c)$^{-2}$.

The secondary hadrons after a string decay were generated randomly. The flavor branching ratios $u:d:s:c = 1:1:0.27:0$ and the quark-diquark formation ratios $(q,\bar{q}):(qq,\overline{qq}) = 1:0.09$.

At string breakup the $q\bar{q}$ pair has zero transverse momentum, but nevertheless, the momenta of the separate quark $\mathbf{p}_t$ and the corresponding antiquark $-\mathbf{p}_t$ were assumed to be distributed according to

$$f_2(\mathbf{p}_t) = \frac{3b_2}{\pi(1+b_2 p_t^2)^4} \ , \tag{27}$$

with $b_2 = 0.7$ (GeV/c)$^{-2}$. The transverse momentum of a hadron consists of the transverse momenta of its quarks.

The choice of b_1 and b_2 is essential for the lower level of the mean transverse momentum of produced hadrons as a function of charged multiplicity (see below).

The longitudinal momentum and energy of the produced hadron were determined through the variable $z = (E+p_\parallel)_h/(E+p_\parallel)_q$. The quantity z was generated by using a distribution of the form

$$f_h^q(z) \sim (1-z)^{\alpha_q^h(p_t)} \ . \tag{28}$$

At $z \to 1$ this function coincides with the fragmentation function $D_q^h(z)$ of q quarks (antiquarks) or qq diquarks (anti-diquarks) into a hadron h. As shown in Ref. [11], the exponent $\alpha_q^h(p_t)$ depends on the flavor of the constituent, on the type of a hadron it is transformed into, and on the transverse momentum of the hadron. The values $\alpha_q^h(p_t)$ were taken in each case from Ref. [11].

If the mass of a string, M_S, were less than $M_0 = M_R + \Delta M_R$, where $\Delta M_R = 0.35$ GeV/c and M_R is the mass of the resonance with the same quark composition as the string, only one break of such a string (cluster) was generated. Its kinematics was determined by the cluster mass and isotropy of the emission of two hadrons.

B. Pseudorapidity distributions

In Fig. 3 we compare the rapidity distributions of experimental data from UA5 [43] at the Intersection Storage Rings CERN (SR) and UA5 [43] at the CERN SPS collider and the Collider Detector at Fermilab (CDF) [44] at the Tevatron with model calculations. We simulated 20 000 inelastic collisions at each energy and reproduced the data. However, as was demonstrated in earlier papers [16], it is also possible to explain the rise of the charged multiplicity plateau with increasing collision energy without semihard collisions.

C. Average transverse momentum

In Fig. 4 the mean transverse momentum is plotted as a function of the negative-charge particle multiplicity in the central rapidity region $|y| \le 2.5$ of $p\bar{p}$ collisions at $\sqrt{s} = 540$ GeV [26] and in $|y| \le 3.25$ at $\sqrt{s} = 1800$ GeV [27,28]. The mean transverse momentum was calculated in the QGSM with the experimental definition

$$\langle p_t \rangle = \frac{1}{N_{\rm ch}} \sum_{i=1}^{N_{\rm ch}} p_t^i \tag{29}$$

separately for each event and then averaged over all

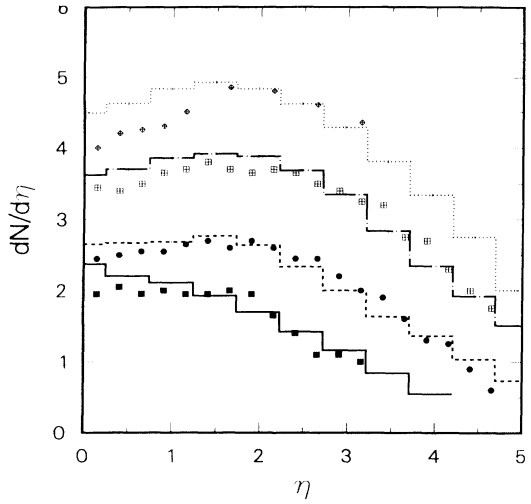

FIG. 3. Pseudorapidity distributions $dN/d\eta$ of charged particles as a function of energy. Histograms are predictions of the QGSM. Experimental UA5 points at $\sqrt{s}=53$, 200, and 900 GeV are taken from Ref. [43], and CDF points at $\sqrt{s}=1800$ GeV are taken from Ref. [44], (solid, dot-dashed, and dotted lines, respectively).

events. Here N_{ch} is the number of charged particles in the given rapidity interval. We simulated 300 000 events at each energy. The dependence of the mean transverse momentum on the charged multiplicity in the absence of semihard gluon scatterings in pp collisions at $\sqrt{s}=31$ GeV (cf. Refs. [21,22]) is shown in Fig. 4 by the dot-dashed line. The mean p_t is determined by the parameters of the intrinsic transverse momentum of partons and string fragmentation. In this case the mean transverse momentum of negative particles decreases with increasing charged-particle multiplicity. Such behavior of the mean p_t as a function of charged multiplicity is consistent with experimental data (see, for example, Ref. [29]) at this energy.

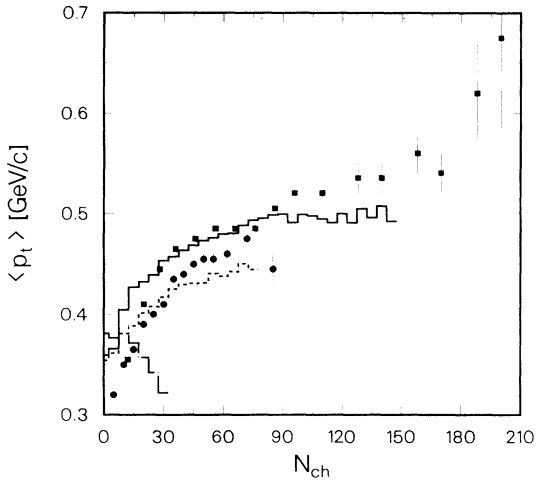

FIG. 4. Average transverse momentum for negative particles produced in the central region of rapidity. Histograms are predictions of the QGSM for the proton-proton collision at $\sqrt{s}=31$ GeV, $|y|<2.0$ (dot-dashed line) and the proton-antiproton collision at $\sqrt{s}=540$ GeV, $|y|<2.5$ (dashed line) and at $\sqrt{s}=1800$ GeV, $|y|<[=3.25$ (solid line), as a function of charged multiplicity. Experimental points at 540 GeV taken from Ref. [26] and at 1800 GeV from Ref. [27].

For higher energy, where the semihard collisions play a role, it is well known that the behavior of the mean p_t is qualitatively different [19], as also seen in data from the SPS collider [26]. There is now an initial rise followed by a plateau with increasing multiplicity. By including semihard scattering, our model predictions approximately agree with the experimental data, as seen from Fig. 4.

The Tevatron experiment [27] extended these measurements to higher multiplicities and observed a second rise in mean p_t as well, although the experimental points have large error bars. As follows from fluid-thermodynamical models [30], in which the transverse momentum is related to flow and temperature [45] and the multiplicity of produced particles to entropy, the signature of a phase transition is a discontinuity in the plot of entropy versus temperature or average transverse momentum versus multiplicity.

As seen from Fig. 4, the inclusion of the semihard collisions is not able to account for a second rise of the mean transverse momentum for charged particles at high multiplicity. At charged multiplicity $N_{ch}>90$, the model somewhat underestimates the experimental values of the mean p_t from the Tevatron. As can be seen in Fig. 5, this is connected with an underestimation in the model of the mean transverse momentum for heavier particles, such as antiprotons.

At $\sqrt{s}=1800$ GeV, the measured [27,28] values of the average transverse momentum $\langle p_t \rangle$ are presented in Fig. 5 as a function of charged multiplicity N_{ch} for $\bar{p}$, π, and K production separately. As seen in Figs. 5(b) and 5(c), the model reproduced the pion and approximately the kaon data [28]. In sharp contrast there is a sizable

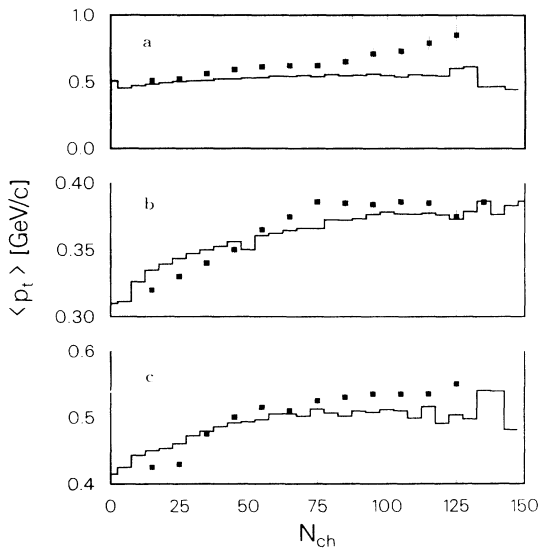

FIG. 5. (a)–(c) Plots of $\langle p_t \rangle$ vs N_{ch} for $\bar{p}$, pions, and kaons, respectively, for particles with $p_t \leq 1.5$ GeV/c. Experimental points are taken from Ref. [28]. Histograms are predictions of the QGSM.

discrepancy between model predictions and the experimental antiproton data, as demonstrated in Fig. 5(a). In our model the rise of the mean hadron transverse momentum with increasing multiplicity is determined by semihard collisions. But antiproton production in semihard collisions is strongly suppressed by the small masses of the final strings and clusters. Our conclusions are identical to the results obtained in Ref. [46], with the dual-parton-model event generator. However, these results should be contrasted to the results obtained in Ref. [47]. They obtain a good fit also to the antiproton data.

D. Strangeness production

The measured [28] ratios K/π and $\bar{p}/\pi^-$, calculated from production cross sections and averaged over the central rapidity region in the Tevatron experiments, are shown in Fig. 6 as a function of charged multiplicity N_{ch}. The ratio K/π appears to increase with multiplicity, reaching a value $K/\pi=0.14$.

The lower level of the model's K/π ratio is mainly determined by the strangeness suppression parameter at the breakup of strings [the dashed histogram in Fig. 6(a)]. Higher multiplicity in an event is connected to a larger number of strings in soft rescatterings and to a larger number of parton showers in semihard gluon-gluon rescatterings. An eventual rise in the K/π ratio in the model as a function of charged multiplicity N_{ch} is determined by the strangeness content of strings produced in soft collisions and the probability of finding strange sea quark pairs in the nucleon. The latter is a free phenomenological parameter of our model. The importance of this parameter is seen in Fig. 6(a), where for the solid histogram there is no suppression of strange sea quark pairs inside the proton, as compared with nonstrange sea quark pairs. For the dashed histogram, the strange sea quark pairs were completely suppressed.

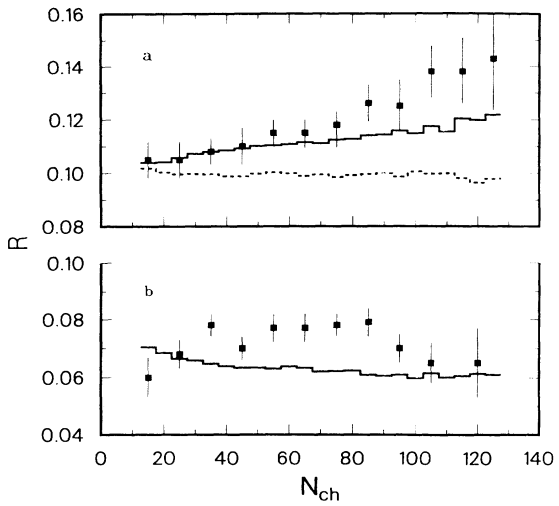

FIG. 6. (a) and (b) Ratios of K/π and $\bar{p}/\pi$, respectively, as a function of charged multiplicity N_{ch}. Experimental points are taken from Ref. [28]. The solid and dashed histograms are predictions of the QGSM without and with complete suppression of the strange sea quarks on the ends of strings originated from the soft collisions.

Inclusion of quark-antiquark semihard scatterings into the strange quark pair final state, in our opinion, cannot improve the description of the experimental rise of the K/π ratio, because the probability of such scatterings is negligibly small as compared with gluon semihard scatterings at small x.

The model ratio $\bar{p}/\pi^-$, which is determined only by the antibaryon suppression parameter at the breakup of strings and clusters, has a rather different behavior as a function of N_{ch} than the experimental ratio.

V. STRING-STRING AND PARTON-PARTON INTERACTIONS

As shown in Fig. 2, the mean number of the soft collisions in central $p\bar{p}$ collisions at $\sqrt{s}=1800$ GeV with impact parameters less than 0.3 fm approximately equals 3.5. For computational reasons we limited the maximum number of soft collisions in a single event to 15. In each soft collision, we produce two strings, which means that we on the average produce 7 strings inside a nucleon-size domain in central collisions, and the maximum number of produced strings reaches 30. Thus the assumption of independent strings is highly questionable, and string-string interactions should be included.

One may attempt to introduce string-string interactions by, for example, allowing strings to merge to create "string ropes" [48,49]. The string tension of a K-fold rope, κ', formed by the K parallel strings, each characterized by the string tension κ separately, is

$$\kappa'=2K\kappa \ . \tag{30}$$

In correspondence with the Schwinger tunneling probability for production of quark and diquark pairs, the strangeness and antibaryon suppression factors and transverse momentum distribution of the quarks and diquarks for a rope differs from those for a string by the larger string tension of a rope. For instance, at the breakup of a rope, the quarks or diquarks will have a transverse mass m_t generated by the distribution

$$P(m_t)=\exp(-\pi m_t^2/\kappa') \ . \tag{31}$$

Thus to form ropes in central collisions appears to be a mechanism capable of explaining a rise in the mean p_t as a function of charged multiplicity for the antibaryons, in particular the antiprotons, as was demonstrated in a recent paper [50]. This will also lead to an enhancement of strangeness production.

Similarly, as seen in Fig. 2 at Tevatron energy, the mean number of semihard collisions approximately equals 5, for impact parameters less than 0.3 fm. Thus we created on the average 10 sources of parton cascades at Tevatron energy in central hadron collisions. In correspondence with the string interactions, rescatterings between partons from different cascades could influence the transverse momentum distribution of produced hadrons and also the enhancement of strangeness production with increasing charged-particle multiplicity.

The effects of string-string interactions and parton-parton scattering will be especially important in nuclear collisions.

Further improvement of the QGSM should consider string-string interactions and the successive rescatterings of partons from different cascades. However, the considered separate division of parton cascades, on the one hand, for the description of semihard collisions and, on the other hand, the string picture for soft collisions based on the eikonal model [21,22] is not unique (see Refs. [19,52]) and contains internal difficulties. As was pointed out in Ref. [51], it is p_t cutoff dependent, and there is a danger that it includes "double counting." Thus, it is not obvious how to include these further interactions.

VI. SUMMARY

In the present work, we incorporated the creation of parton cascades into the Monte Carlo quark-gluon string model [16,17], aiming at a description of hadron-nucleon, hadron-nucleus, and nucleus-nucleus collisions at higher energies than before.

As an example, we have demonstrated the importance of semihard rescatterings of gluons for proton-antiproton collisions at collider energies. The observable quantities, such as the mean p_t for pions and kaons as a function of the charged multiplicity in the central rapidity range, are qualitatively explained by the model.

However, the inclusion of the semihard gluon-gluon scatterings is not sufficient to explain the rise of the mean transverse momentum with multiplicity for heavier particles such as antiprotons, and it does not influence the rise of the ratios K/π and $\bar{p}/\pi^-$ with increasing charged-particle multiplicity.

ACKNOWLEDGMENTS

Enlightening discussions with Carlos Pajares, Joseph Kapusta, and Larry McLerran are gratefully acknowledged. This work was supported by the Norwegian Research Council for Science and Humanities (NAVF), and by the U.S. Department of Energy under Grant No. DE-FG02-87ER40328.

[1] W. M. Geist, D. Drijard, A. Putzer, R. Sosnovski, and D. Wegener, Phys. Rep. **197**, 264 (1990).

[2] H. U. Bengtsson and T. S. Sjostrand, Comput. Phys. Commun. **46**, 43 (1987).

[3] F. E. Paige and S. D. Protopopescu, in *Physics of the Superconducting Super Collider, Snowmass, 1986,* Proceedings of the Summer Study, Snowmass, Colorado, 1986, edited by R. Donaldson and J. Marx (Division of Particles and Fields of the APS, New York, 1987), p. 320.

[4] K. Sailer, W. Greiner, and B. Müller, in *Quark-Gluon Plasma,* edited by R. Hwa, Advanced Series on Directions in High Energy Physics, Vol. 6 (World Scientific, Singapore, 1990), p. 299.

[5] B. Andersson, G. Gustafson, and B. Nilsson-Almquist, Nucl. Phys. **B281**, 289 (1987).

[6] M. Gyulassy, CERN Report No. TH. 4794/87, 1987 (unpublished).

[7] G. Cohen-Tannoudji, A. El. Hassouni, J. Kalinovski, and R. Peschanski, Phys. Rev. D **19**, 3397 (1979).

[8] A. Capella, U. Sukhatme, C. I. Tan, and J. Tran Thanh Van, Phys. Lett. **81B**, 68 (1979); Z. Phys. C **3**, 329 (1980); A. Capella and J. Tran Thanh Van, *ibid.* **10**, 210 (1981); Phys. Lett. **114B**, 450 (1982); A. Capella, C. Merino, H. J. Möhring, J. Ranft, and J. Tran Thanh Van, in *Quark Matter '90,* Proceedings of the Eighth International Conference on Ultra-Relativistic Nucleus-Nucleus Collisions, Menton, France, 1990, edited by J. P. Blaizot, C. Gerschel, B. Pirc, and A. Romana [Nucl. Phys. **A525**, 493c (1991)].

[9] A. B. Kaidalov, Phys. Lett. **116B**, 459 (1982); A. B. Kaidalov and K. A. TerMartirosyan, *ibid.* **117B**, 247 (1982); Yad. Fiz. **39**, 1545 (1984) [Sov. J. Nucl. Phys. **39**, 979 (1984)]; A. B. Kaidalov, *ibid.* **45**, 1452 (1987) [**45**, 902 (1987)].

[10] A. V. Batunin, A. K. Likhoded, and A. N. Tolstenkov, Yad. Fiz. **42**, 424 (1985) [Sov. J. Nucl. Phys. **42**, 268 (1985)]; A. V. Batunin and A. N. Tolstenkov, *ibid.* **42**, 970 (1985) [**42**, 616 (1985)].

[11] A. B. Kaidalov and O. I. Piskunova, Z. Phys. C **27**, 145 (1986).

[12] P. Aurenche, F. W. Bopp, and J. Ranft, Phys. Rev. D **33**, 1867 (1986).

[13] J. Ranft, P. Aurenche, and F. W. Bopp, Z. Phys. C **26**, 279 (1984).

[14] T. P. Pansart, in *Quark Matter '86,* Proceedings of the Fifth International Conference on Ultra-Relativistic Nucleus-Nucleus Collisions-Quark Matter, Asilomar, California, 1987, edited by L. Schroeder and M. Gyulassy [Nucl. Phys. **A461**, 521 (1987)].

[15] K. Werner, in *Quark Matter '90* [8], p. 501c.

[16] N. S. Amelin and L. V. Bravina, Yad. Fiz. **51**, 211 (1990) [Sov. J. Phys. **51**, 133 (1990)]; N. S. Amelin, L. V. Bravina, and L. N. Smirnova, *ibid.* **50**, 1705 (1989) [**50**, 1058 (1989)]; **51**, 892 (1990) [**51**, 567 (1990)]; N. S. Amelin, L. V. Bravina, L. I. Sarycheva, and L. N. Smirnova, *ibid.* **51**, 841 (1990) [**51**, 535 (1990)].

[17] N. S. Amelin, K. K. Gudima, and V. D. Toneev, Yad. Fiz. **51**, 512 (1990) [Sov. J. Nucl. Phys. **51**, 327 (1990)]; **51**, 1730 (1990) [**51**, 1093 (1990)]; N. S. Amelin, K. K. Gudima, S. Yu. Sivoklokov, and V. D. Toneev, *ibid.* **52**, 272 (1990) [**52**, 172 (1990)].

[18] L. V. Gribov, E. M. Levin, and M. G. Ryskin, Phys. Rep. **100**, 1 (1983).

[19] T. S. Sjostrand and M. van Zijl, Phys. Rev. D **36**, 2019 (1987).

[20] L. Durand and H. Pi, Phys. Rev. Lett. **58**, 303 (1987); W. R. Chen and R. C. Hwa, Phys. Rev. D **36**, 760 (1987); X. N. Wang and R. C. Hwa, *ibid.* **39**, 187 (1989).

[21] A. Capella, J. Tran Thanh Van, and J. Kwiecinski, Phys. Rev. Lett. **58**, 2015 (1987).

[22] V. Innocente, A. Capella, and J. Tran Thanh Van, Phys. Lett. B **213**, 81 (1988).

[23] K. Hahn and J. Ranft, Phys. Rev. D **41**, 1463 (1990).

[24] D. H. Boal, Phys. Rev. C **33**, 2206 (1986); K. Geiger and B. Müller, in *Proceedings of the Fourth Workshop on Experiments and Detectors for RHIC,* Upton, New York, 1990, edited by M. Fatyga and B. Moskowitz (BNL Report No. 52262, Upton, NY, 1990), p. 55.

[25] K. Geiger and B. Müller, Duke University Report No. DUK-TH-90-15, 1991 (unpublished).
[26] UA1 Collaboration, G. Arnison *et al.*, Phys. Lett. **118B**, 167 (1982).
[27] T. Alexopoulos *et al.*, Phys. Rev. Lett. **60**, 1622 (1988).
[28] T. Alexopoulos *et al.*, Phys. Rev. Lett. **64**, 991 (1990).
[29] A. Breakstone *et al.*, Phys. Lett. **132B**, 458 (1983).
[30] E. V. Shuryak and O. V. Zhirov, Phys. Lett. **89B**, 253 (1980); L. Van Hove, *ibid.* **118B**, 138 (1982).
[31] P. Koch, B. Müller, and J. Rafelski, Phys. Rep. **142**, 167 (1986).
[32] B. I. Ermolaev and V. S. Fadin, Pis'ma Zh. Eksp. Teor. Fiz. **33**, 285 (1981) [JETP Lett. **33**, 269 (1981)]; A. H. Mueller, Phys. Lett. **104B**, 161 (1981); G. Marchesini and B. R. Weber, Nucl. Phys. **B238**, 1 (1984).
[33] E. Eichten, I. Hinchliffe, K. Lane, and C. Quigg, Rev. Mod. Phys. **56**, 579 (1984); **58**, 1065 (1986).
[34] B. L. Combrige, J. Kripfganz, and J. Ranft, Phys. Lett. **70B**, 234 (1977); R. Cutler and D. Sivers, Phys. Rev. D **17**, 196 (1978).
[35] G. C. Fox and S. Wolfram, Nucl. Phys. **B168**, 285 (1980).
[36] R. D. Field, *Application of Perturbative QCD,* Frontiers in Physics, Vol. 77 (Addison-Wesley, Redwood City, CA, 1978), p. 196.
[37] G. Altarelli and G. Parisi, Nucl. Phys. **B126**, 298 (1977).
[38] R. D. Field and S. Wolfram, Nucl. Phys. **B213**, 65 (1983).
[39] D. Amati and G. Veneziano, Phys. Lett. **83B**, 87 (1979).
[40] B. R. Webber, Nucl. Phys. **B238**, 492 (1984); Annu. Rev. Nucl. Part. Sci. **36**, 253 (1986).
[41] A. Bialas and M. Gyulassy, Nucl. Phys. **B291**, 793 (1987).
[42] G. Gustafson, Z. Phys. C **15**, 155 (1982).
[43] UA5 Collaboration, G. J. Alner *et al.*, Nucl. Phys. **B335**, 261 (1986).
[44] CDF Collaboration, F. Abe *et al.*, Phys. Rev. D **41**, 2330 (1990).
[45] L. P. Csernai, A. K. Holme, and E. F. Staubo, in *The Nuclear Equation of State, Part B: QCD and the Formation of the Quark-Gluon Plasma,* Proceedings of the NATO Advanced Study Institute, Peniscola, Spain, 1989, edited by W. Greiner and H. Stöcker, NATO ASI Series B: Physics, Vol. 216 (Plenum, New York, 1990), pp. 369–384.
[46] F. W. Bopp, A. Capella, J. Ranft, and J. Tran Thanh Van, Z. Phys. C **51**, 99 (1991).
[47] X.-N. Wang and M. Gyulassy, Phys. Rev. D **45**, 844 (1992).
[48] T. S. Biro, H. B. Nielsen, and J. Knoll, Nucl. Phys. **B245**, 449 (1984); M. Gyulassy and A. Iwazaki, Phys. Lett. **165B**, 157 (1985); A. K. Kerman, T. Matsui, and B. Svetitsky, Phys. Rev. Lett. **56**, 219 (1986).
[49] M. Gyulassy, in *Quark-Gluon Plasma* [4], p. 223.
[50] C. Merino, C. Pajares, and J. Ranft (private communication).
[51] B. Andersson, Phys. Scr. **T32**, 61 (1989).
[52] X. N. Wang, Phys. Rev. D **43**, 104 (1991).